Sveučilište u Rijeci
University of Rijeka
https://www.uniri.hr

Polytechnica: Journal of Technology Education, Volume 9, Number 2 (2025)
Politehnika: Časopis za tehnički odgoj i obrazovanje, Svezak 9, Broj 2 (2025)

Politehnika
Polytechnica
https://www.politehnika.uniri.hr
e-mail: cte@uniri.hr

DOI: https://doi.org/10.36978/cte.9.2.2

Stručni članak
Professional paper

Static and Kinematic Analysis of the Scissor Lift STEM toy

Alma Žiga, Lamija Mešeljević, Amra Talić-Čikmiš

Faculty of Mechanical Engineering

University of Zenica

Fakultetska 1, 72000 Zenica, B&H

alma.ziga@unze.ba, lamija.meseljevic@unze.ba,
amra.talic.cikmis@unze.ba

Abstract

STEM is an acronym that stands for Science, Technology, Engineering, and Mathematics. It represents a broad educational focus aimed at developing problem-solving skills, critical thinking, and innovation. STEM education integrates these four disciplines to encourage students to apply theoretical knowledge to real-world challenges, fostering a deeper understanding of how various fields interconnect. This study focuses on the static and kinematic analysis of a scissor lift STEM toy, utilizing both analytical methods and design software simulations. The first objective is to develop a detailed 3D model of the toy's scissor lift mechanism based on physical measurements and observations. The model is then analysed using computer-aided design (CAD) software to evaluate its static equilibrium and motion characteristics. The results from the software simulations are compared with the analytical findings. The study contributes to understanding the mechanical behaviour of scissor lift mechanisms and demonstrates the advantages and limitations of different analysis approaches.

Keywords: *STEM toys; scissor lift; statics; kinematics; design software.*

1 Introduction

In modern STEM education, integrating hands-on projects with theoretical concepts is essential for cultivating practical engineering skills. The scissor lift mechanism, commonly used in industrial and construction applications, has been adapted into a STEM toy, offering an accessible platform to explore fundamental mechanical principles.

The scissor lift mechanism, Figure 1, is a fascinating engineering structure that utilizes a series of interconnected, pivoting arms arranged in a crisscross, or pantograph, configuration. As the arms expand and contract, they convert horizontal movement or an applied force into vertical displacement, allowing a platform to raise or lower. This design offers several advantages:

Compactness and Efficiency: The scissor configuration enables a large vertical lift within a relatively small footprint, making it ideal for environments with limited space.

Force Distribution: The mechanical advantage inherent in the crossed arms distributes loads evenly, enhancing stability and supporting significant weight.

Versatility in Actuation: While industrial scissor lifts often employ hydraulic or pneumatic systems for motion control, simplified versions—such as those found in STEM toys—may use manual inputs or basic mechanical linkages. This adaptability makes the mechanism an excellent educational tool.

Complex Kinematics: The interplay between rotational and translational motions in the mechanism presents rich opportunities for both static and kinematic analysis. Understanding these interactions deepens insights into the dynamics of mechanical systems and reinforces core engineering principles.

Since the lifting platforms that use scissors mechanism are so commonly used, it is no surprise that a lot of different authors approached the problem of finding the optimal solution for the construction of the devices. The analysis of scissor lift platforms is a multidisciplinary area encompassing both static (force, stress, stability) and kinematic (motion, displacement, velocity, acceleration) considerations, crucial for ensuring safe and efficient design and operation. Researchers employ various mathematical modelling techniques to represent the complex geometry and interconnected linkages of scissor mechanisms. The increasing availability and sophistication of computational tools and simulation software, such as MATHCAD, Working Model, ANSYS, SolidWorks, and finite element analysis (FEA) packages, have become integral to analysing the behaviour and structural integrity of these systems under diverse loading conditions.

Figure 1. 3D model of a scissor lift mechanism

A significant portion of the literature focuses on optimizing the structural design of scissor lift components. This includes determining optimal dimensions, material selection, and joint configurations to maximize load-bearing capacity while minimizing weight and material usage. Methodologies like the Harris Hawks Optimization (HHO) algorithm in (Todorović, Zdravković, Savković, Marković, & Pavlović, 2021) and parametric analysis in (Dang, Nguyen, & Nguyen, 2023) have been applied to achieve these optimization goals.

Kinematic analysis is essential for understanding the motion characteristics of the platform, including its lifting height, velocity profiles, and acceleration. Several studies such as [(Dang, Nguyen, & Nguyen, 2023), (Cirak, 2019), (Doçi, Lajqi, & Bibaj, 2021)] aim to refine the understanding of these relationships to ensure smooth and controlled lifting operations. A critical aspect explored is the minimization of oscillations that can occur during lifting, particularly when handling maximum loads, as these oscillations can compromise safety and operational efficiency, (Doçi, Lajqi, & Bibaj, 2021).

While many analyses simplify the problem by focusing on static behaviour under the assumption of low lifting speeds and negligible inertia forces as presented in (Todorović, Zdravković, Savković, Marković, & Pavlović, 2021) and (Cirak, 2019), the importance of dynamic analysis is increasingly recognized. Dynamic studies aim to model and predict the time-dependent behaviour of scissor lifts, including the influence of inertia, damping, and external disturbances. This is particularly relevant when considering motion regulation and control strategies to achieve desired lifting speeds and minimize unwanted vibrations as shown in (Doçi, Lajqi, & Bibaj, 2021) and (Islam, Yin, Shengqi , & Rolland, 2014). The forces exerted by hydraulic cylinders during lifting are a key parameter investigated in dynamic analyses, (Doçi, Lajqi, & Bibaj, 2021).

Furthermore, research explores specific design configurations, such as double-layer scissor lifts in (Dang, Nguyen, & Nguyen, 2023) and lifts for specialized applications like magazine lifting mechanisms in (Hua-Ting, Chen, Ke, Chen-Xu, & Lei, 2024). These studies often involve tailored mathematical models and simulations to address the unique challenges and requirements of these designs. The role of actuator positioning and its impact on the mechanical advantage and force output of scissor lifts is also a subject of investigation in (Saxena, 2016).

This study focuses on developing a detailed 3D model of a scissor lift toy in SolidWorks to perform both static and kinematic analyses. The static analysis examines force distributions and equilibrium conditions to ensure stability, while the kinematic analysis investigates motion parameters such as displacement, velocity, and acceleration during operation. The same static and kinematic analyses were also conducted analytically using Wolfram Mathematica software to plot diagrams during platform ascent. The relatively simple motion of this scissor mechanism allows for analytical analysis, unlike the more complex mechanism described in (Žiga, Ćaro, & Mešeljević, 2024), which necessitated a purely numerical approach. This simplicity enables the utilization of mathematical software to obtain plots of various parameters and to compare them with diagrams obtained in motion analysis software.

By employing both traditional analytical methods and advanced software simulations, the research aims to validate computational models against theoretical predictions. This dual approach not only highlights the strengths and limitations of each method but also reinforces the educational value of applying real-world engineering analysis to simplified models. Ultimately, the study seeks to enhance our understanding of mechanical interactions within scissor lift mechanisms and demonstrate how such models can be effectively used in STEM curricula to bridge the gap between theory and practice.

2 Static analysis

The construction solution of the scissor lift mechanism being analysed is shown in Figure 2. The mechanism consists of an upper platform on which the load *W* is applied. The platform is connected to the scissor mechanism via pin *B* and slider *A*. The distance between pin *B* and slider *A* is denoted by *s*, and its value changes as the slider moves. The scissor mechanism is composed of four equally long levers (*AE*, *BD*, *DP* and *EN*) connected at their midpoints by pins *C* and *M*. The base is connected to the scissor mechanism via pin *P* and piston *N*. Free body diagrams of the described mechanism are shown in Figure 3, 4 and 5.

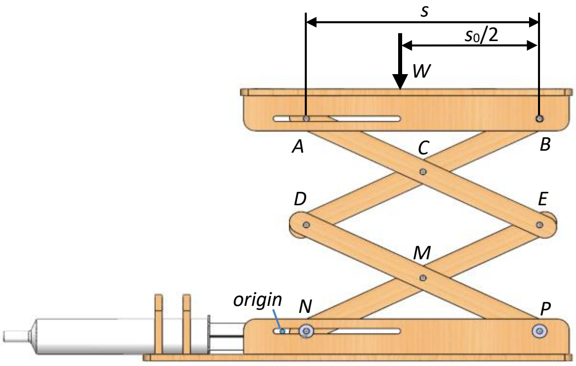

Figure 2. Illustration of lifting platform with scissor mechanism

Given that the lifting speed, weight and acceleration of the platform are not high, inertia forces can be neglected, and the entire construction can be considered static. The static equations can be determined for the system depicted in Figure 3, 4, 5.

Static equations for the platform *AB*, Figure 3:

$$\sum Y_i = 0:\ F_A + F_B - W = 0 \qquad (1)$$
$$\sum M_B = 0 : W \cdot s_0/2 - F_A \cdot s = 0 \qquad (2)$$

Static equations for the beam *AE*, Figure 4:

$$\sum X_i = 0:\ F_{Cx} + F_{Ex} = 0 \qquad (3)$$
$$\sum Y_i = 0:\ -F_A + F_{Cy} + F_{Ey} = 0 \qquad (4)$$
$$\sum M_E = 0:$$
$$F_A \cdot l cos\theta - F_{Cy} \cdot \frac{l}{2} cos\theta - F_{Cx} \cdot \frac{l}{2} sin\theta = 0 \qquad (5)$$

Static equations for the beam *BD*, Figure 4:

$$\sum X_i = 0:\ -F_{Cx} - F_{Dx} = 0 \qquad (6)$$
$$\sum Y_i = 0:\ -F_B - F_{Cy} + F_{Dy} = 0 \qquad (7)$$
$$\sum M_D = 0:$$
$$-F_B \cdot l cos\theta - F_{Cy} \cdot \frac{l}{2} cos\theta + F_{Cx} \cdot \frac{l}{2} sin\theta = 0 \qquad (8)$$

Static equations for the beam *DP*, Figure 5:

$$\sum X_i = 0:\ F_{Dx} + F_{Mx} + F_{Px} = 0 \qquad (9)$$
$$\sum Y_i = 0:\ -F_{Dy} + F_{My} + F_{Py} = 0 \qquad (10)$$
$$\sum M_P = 0:$$
$$F_{Dy} \cdot l cos\theta - F_{Dx} \cdot l sin\theta - F_{My} \cdot \frac{l}{2} cos\theta$$
$$-F_{Mx} \cdot \frac{l}{2} sin\theta = 0 \qquad (11)$$

Static equations for the beam *EN*, Figure 5:

$$\sum X_i = 0:\ -F_{Mx} - F_{Ex} - F_{Nx} = 0 \qquad (12)$$
$$\sum Y_i = 0:\ F_{Ny} - F_{My} - F_{Ey} = 0 \qquad (13)$$
$$\sum M_N = 0:$$
$$-F_{Ey} \cdot l cos\theta + F_{Ex} \cdot l sin\theta - F_{My} \cdot \frac{l}{2} cos\theta$$
$$+F_{Mx} \cdot \frac{l}{2} sin\theta = 0 \qquad (14)$$

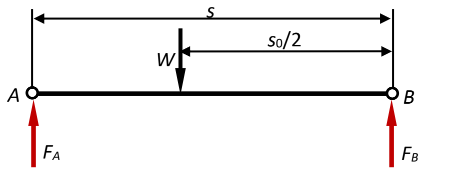

Figure 3. Free body diagram of mechanism for the platform *AB*

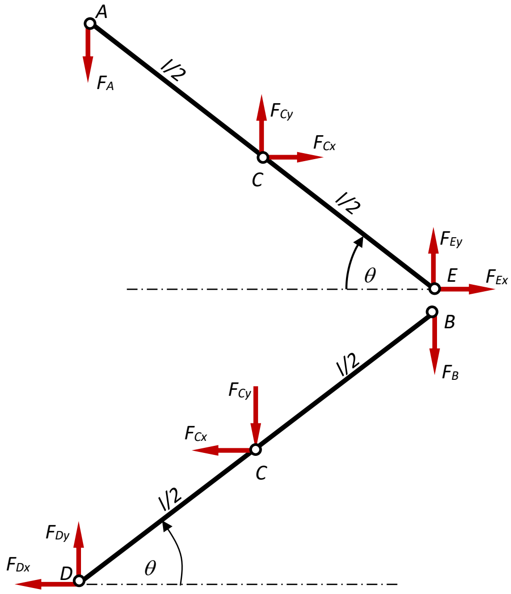

Figure 4. Free body diagram of mechanism for beams *AB* and *BD*

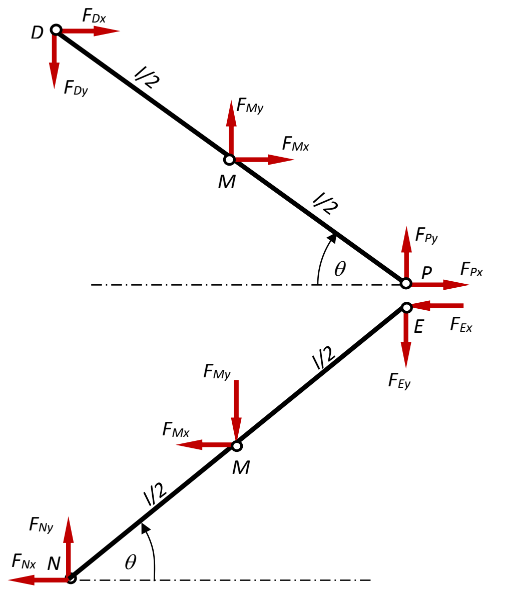

Figure 5. Free body diagram of mechanism for beams *EN* and *DP*

From equations 1 and 2 it follows that $F_A = W \cdot s_0/(2s)$ and $F_B = W - W \cdot s_0/(2s)$.

Equations 3-14 can be written in matrix form, which is suitable for solving with the use of computer:

$$\begin{pmatrix} 1 & 0 & 0 & 0 & 1 & 0 & 0 & 0 & 0 & 0 & 0 & 0 \\ 0 & 1 & 0 & 0 & 0 & 1 & 0 & 0 & 0 & 0 & 0 & 0 \\ \frac{1}{2}*\mathrm{Sin}[\theta] & \frac{1}{2}*\mathrm{Cos}[\theta] & 0 & 0 & 0 & 0 & 0 & 0 & 0 & 0 & 0 & 0 \\ -1 & 0 & -1 & 0 & 0 & 0 & 0 & 0 & 0 & 0 & 0 & 0 \\ 0 & -1 & 0 & 1 & 0 & 0 & 0 & 0 & 0 & 0 & 0 & 0 \\ \frac{1}{2}*\mathrm{Sin}[\theta] & -\frac{1}{2}*\mathrm{Cos}[\theta] & 0 & 0 & 0 & 0 & 0 & 0 & 0 & 0 & 0 & 0 \\ 0 & 0 & 1 & 0 & 0 & 0 & 1 & 0 & 1 & 0 & 0 & 0 \\ 0 & 0 & 0 & -1 & 0 & 0 & 0 & 1 & 0 & 1 & 0 & 0 \\ 0 & 0 & -1*\mathrm{Sin}[\theta] & 1*\mathrm{Cos}[\theta] & 0 & 0 & \frac{-1}{2}*\mathrm{Sin}[\theta] & -\frac{1}{2}*\mathrm{Cos}[\theta] & 0 & 0 & 0 & 0 \\ 0 & 0 & 0 & 0 & -1 & 0 & -1 & 0 & 0 & 0 & -1 & 0 \\ 0 & 0 & 0 & 0 & 0 & -1 & 0 & -1 & 0 & 0 & 0 & 1 \\ 0 & 0 & 0 & 0 & 1*\mathrm{Sin}[\theta] & 1*\mathrm{Cos}[\theta] & \frac{1}{2}*\mathrm{Sin}[\theta] & -\frac{1}{2}*\mathrm{Cos}[\theta] & 0 & 0 & 0 & 0 \end{pmatrix} \cdot \begin{pmatrix} Fcx \\ Fcy \\ Fdx \\ Fdy \\ Fex \\ Fey \\ Fmx \\ Fmy \\ Fpx \\ Fpy \\ Fnx \\ Fny \end{pmatrix} == \begin{pmatrix} 0 \\ Fa \\ Fa*1*\mathrm{Cos}[\theta] \\ 0 \\ Fb \\ Fb*1*\mathrm{Cos}[\theta] \\ 0 \\ 0 \\ 0 \\ 0 \\ 0 \\ 0 \end{pmatrix} \quad (15)$$

The total weight on the top platform is W = 2 N, and this weight is distributed across both the front and rear scissor mechanisms, Figure 1. The function s is: $s = 86.8 - 4t^2 + \frac{2}{3}t^3$ and is described in detail in the next section, where s_0 = 86.8 mm at the start of the lifting and l = 87.5 mm is the length of one scissor bar. For the numerical analysis, the weight is not divided between these two mechanisms because the SolidWorks model yields the total reaction magnitude on one axle, which encompasses two mirrored scissors. Therefore, on a single scissor pin, half the calculated reaction value will be acting. In the numerical analysis, the weight is applied linearly from zero to its maximum value of 2 N over a duration of 0.1 seconds. Consequently, all SolidWorks static diagrams show a value rising from zero to a level that closely approximates the analytical findings at the start of the ascent. This weight value then remains constant for the remaining 4 s of the lifting period.

2.1 Results

Once the system of equations (15) is solved, the reaction forces in the joints can be determined and represented using diagrams for the defined time interval of 4 seconds. The results from both the analytical and numerical methods are shown in Figures 6-9. The labels of all reaction forces are not fully consistent in the equations and diagrams and the markings on the coordinate axes (t or time) and units of measurement are not consistent (s or sec) because analytical diagrams are obtained in mathematical software, and numerical ones in SolidWorks software, and these diagrams are copied from these software with all limitations in the possibilities of indexing forces and marking time.

At point N, there is a movable support. The force F_{Ny} is the vertical reaction force, and F_{Nx} is the piston force. F_N is the total force at point N. In this case, where the total load is W = 2 N, the difference between the total force F_N and the piston force F_{Nx} is negligible. The value of F_{Ny} changes from 1 to 1.33 N during the lifting period.

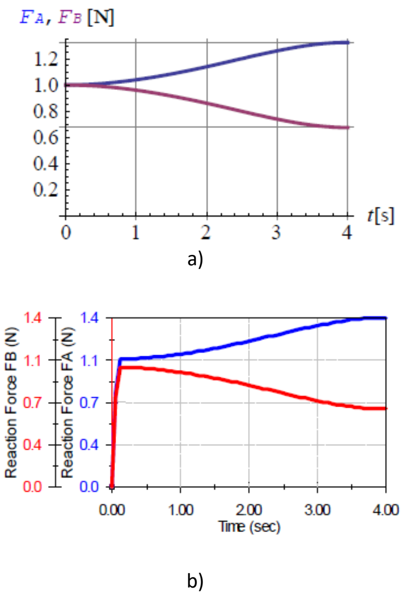

Figure 6. Reaction forces in the pin B and slider A obtained by a) analytical method; b) numerical method

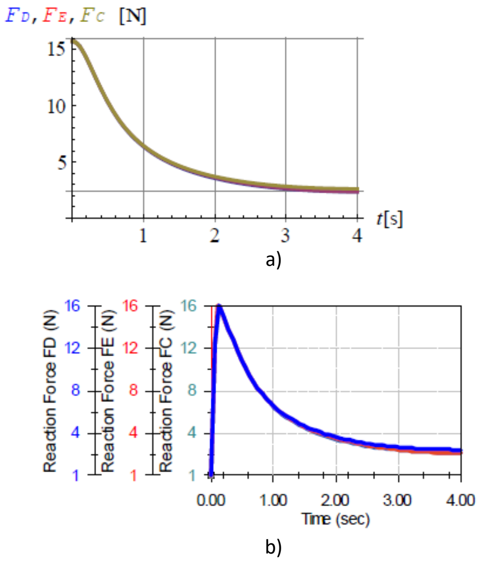

Figure 7. Reaction forces in pins C, D and E obtained by a) analytical method; b) numerical method

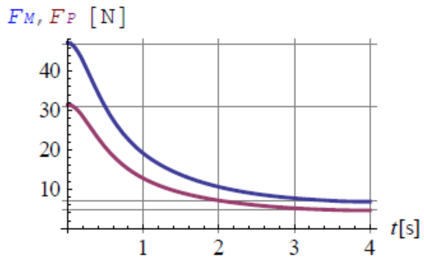

a)

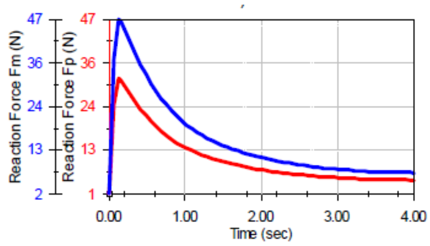

b)

Figure 8. Reaction forces in pins *M* and *P* obtained by a) analytical method; b) numerical method

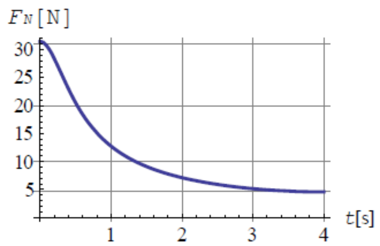

a)

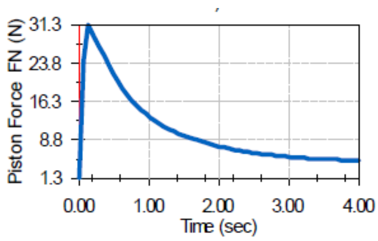

b)

Figure 9. Piston force F_N obtained by a) analytical method; b) numerical method

3 Kinematic analysis

In the scissor lift mechanism, the linear motion of a piston, Figure 10, is transformed into the vertical movement of the platform through the lever's floating motion. By setting a velocity function for the piston to be a second order parabola, the corresponding displacement (*s*) and height (*h*) functions are derived. Adopted function as piston velocity is:

$$v_{piston} = 8t - 2t^2 \left[\frac{mm}{s}\right] \quad (16)$$

Piston displacement will be:

$$s = -\int v_{piston}\, dt = -\int (8t - 2t^2) dt \quad (17)$$

$$s = 86.8 - 4t^2 + \frac{2}{3}t^3 \quad (18)$$

Where s_0 = 86.8 mm at the start of the lifting and l = 87.5 mm is the length of one scissor bar.

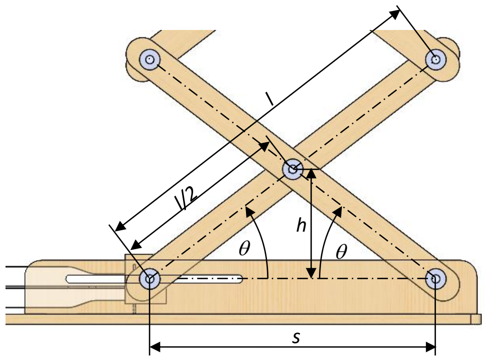

Figure 10. The scissor lift STEM toy

The height *h* is obtained by applying Pythagoras theorem:

$$h = \frac{1}{2}\sqrt{l^2 - s^2} \quad (19)$$

Equations 16-19 allow us to determine the displacement and velocity of the scissor lift platform.

Figure 11 shows diagrams for displacement, velocity and acceleration of the piston obtained in SolidWorks using Motion Analysis study. For this analysis, linear motor motion is assumed, with adopted piston displacement as expression: $-4t^2 + \frac{2}{3}t^3$.

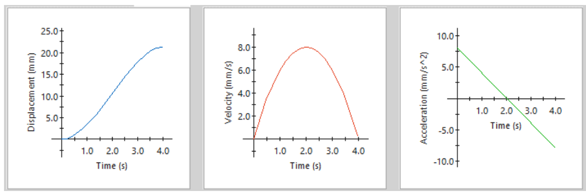

Figure 11. Diagrams for displacement, velocity and acceleration of the piston obtained in SolidWorks using Motion Analysis study

Piston velocity and the distance *s* from the Figure 10 are obtained in the software. The origin of the coordinate system is set at the centre of the axle that aligns with the piston head. The results from both the analytical and numerical methods are shown in Figures 12-14.

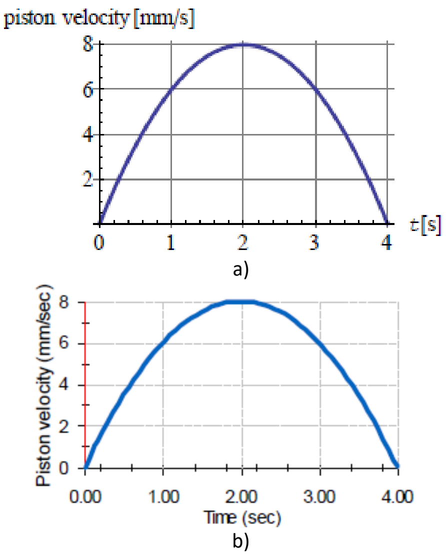

Figure 12. Piston velocity obtained by a) analytical method; b) numerical method

According to Figure 10, platform displacement (P_d) will be:

$$P_d = 4 \cdot h \tag{20}$$

Applying previously defined equations (18) and (19), platform displacement can be defined as:

$$P_d = 2\sqrt{87.5^2 - \left(86.8 - 4t^2 + \frac{2}{3}t^3\right)^2}\ [mm] \tag{21}$$

Platform position at the beginning (0 s) is $P_{d\,0}$ = 22.09 mm, and at the end of the observed time interval (4s) is $P_{d\,4}$ =116.11 mm.

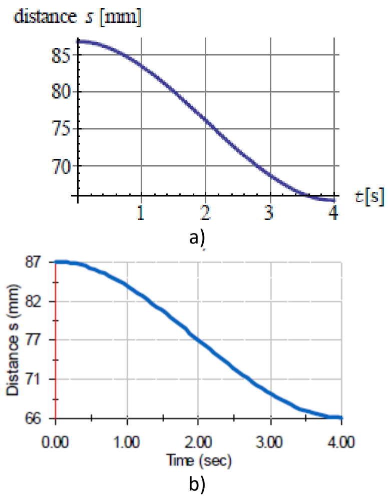

Figure 13. Distance *s* obtained by a) analytical method; b) numerical method

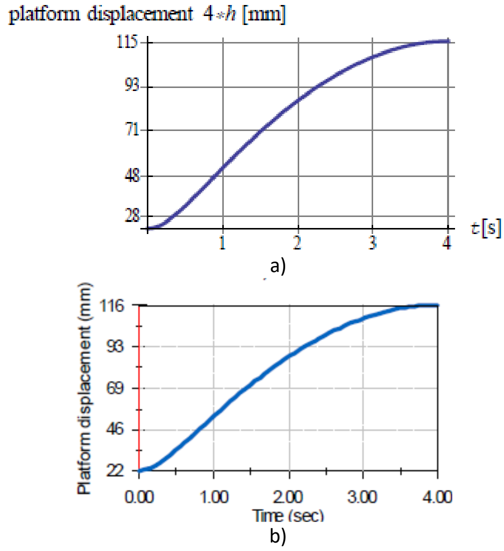

Figure 14. Platform displacement obtained by a) analytical method; b) numerical method

The results of analytical, as well as numerical method for platform displacement, are shown in Figure 14.

Velocity of platform can be defined as:

$$v_p = \frac{dP_d}{dt} = \frac{d}{dt}\left(2\sqrt{87.5^2 - \left(86.8 - 4t^2 + \frac{2}{3}t^3\right)^2}\right) \tag{20}$$

$$v_p = \frac{-2\left(86.8-4t^2+\frac{2}{3}t^3\right)\left(-8t+2t^2\right)}{\sqrt{87.5^2-\left(86.8-4t^2+\frac{2}{3}t^3\right)^2}}\ [mm/s] \tag{21}$$

The results of analytical, as well as numerical method for platform velocity, are shown in Figure 15.

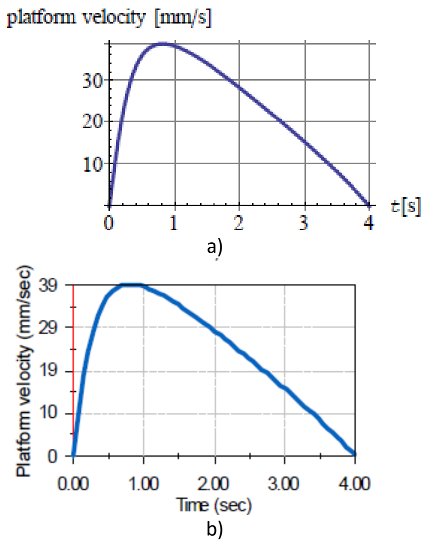

Figure 15. Platform velocity obtained by a) analytical method; b) numerical method

Maximum platform velocity is for t = 0,815 s, where platform acceleration is zero, Figure 16.

$$v_{pmax\,(t=0{,}815s)} = 38{,}6513\ mm/s$$

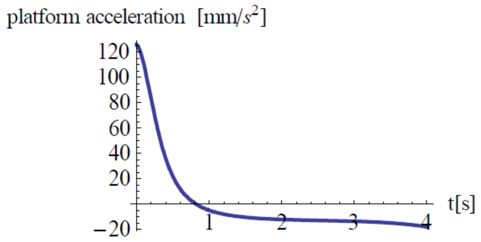

Figure 16. Platform acceleration obtained by analytical method

4 Conclusion

It can be concluded that the results of the static and kinematic analysis of the scissor lift stem toy obtained by software and analytical methods agree to a large extent.

The scissor lift platform has a maximum velocity about 4.5 times higher than the maximum velocity of the piston and the platform has about 4.5 times the displacement in relation to the piston. This information best describes the usefulness of this mechanism and explains why it is used in practice.

The comparison between theoretical calculations and software-generated results demonstrates a high level of accuracy, confirming the reliability of the applied methodologies. The findings contribute to a better understanding of the mechanical behaviour of scissor lift mechanisms and highlight the effectiveness of CAD tools in engineering education. Additionally, this research underscores the importance of STEM-based learning through hands-on applications, reinforcing the connection between theoretical knowledge and practical problem-solving. Future work may include further optimization of the model, experimental validation, and exploration of alternative materials to enhance the toy's performance and educational value.

References

Cirak, B. (2019). Dynamic Analysis of the Hydraulic Scissors Lift Mechanism. *International Journal of Science and Research (IJSR)*. doi:10.21275/ART20203311

Ciupan, C., Ciupan, E., & Pop, E. (2019). Algorithm for designing a hydraulic scissor lifting platform. *MATEC Web of Conferences.* doi:https://doi.org/10.1051/matecconf/2019299 03012

Dang, A.-T., Nguyen, D.-V., & Nguyen, D.-N. (2023). Applying parametric analysis in enhancing performance for double-layer scissor lifts. *Strojniški vestnik-Journal of Mechanical Engineering*, 299-307. doi:10.5545/sv-jme.2023.539

Doçi, I., Lajqi, S., & Bibaj, B. (2021). Scissor lift dynamic analysis and motion regulation for the case of lifting with maximum load. *Trans Motauto World*, 38-42.

Hua-Ting, W., Chen, C., Ke, H., Chen-Xu, H., & Lei, C. (2024). Research on the design of the magazine lifting mechanism based on double scissor structure. *Journal of Physics: Conference Series, 2891*(16). doi:10.1088/1742-6596/2891/16/162004

Islam, M., Yin, C., Shengqi , J., & Rolland, L. (2014). Dynamic analysis of scissor lift mechanism through bond graph modeling. *2014 IEEE/ASME International Conference on Advanced Intelligent Mechatronics* (pp. 1393-1399). IEEE.

Momin, G., Hatti, R., Dalvi, K., Bargi, F., & Devare, R. (2015). Design, manufacturing & analysis of hydraulic scissor lift. *International Journal of Engineering Research and General Science*.

Saxena, A. (2016). *Deriving a Generalized, Actuator Position-Independent Expression for the Force Output of a Scissor Lift.* arXiv preprint arXiv:1611.10182.

Todorović, M., Zdravković, N. B., Savković, M., Marković, G., & Pavlović, G. (2021). Optimization of scissor mechanism lifting platform members using HHO method. *THE EIGHTH INTERNATIONAL CONFERENCE TRANSPORT AND LOGISTICS, til* (pp. 91-96). Niš: UNIVERSITY OF NIS, FACULTY OF MECHANICAL ENGINEERING.

Yimer, W., & Wang, Y. (2019). Design, analysis and manufacturing of double scissors lift elevated by one hydraulic cylinder. *International Journal of Engineering Research & Technology*.

Žiga, A., Ćaro, A., & Mešeljević, L. (2024). 3D PRINTED TOY WATCH WITH MECHANICAL IRIS. *New Technologies, Development and Applications, NT-2024.* Cham: Springer Nature Switzerland.